Journal of Applied Polymer Science

Biodegradable Poly (butylene succinate-co-cyclohexanedimethylene succinate): Synthesis, Crystallization, Morphology, and Rheology

Tong Wan, Tao Du, Shuang Liao
College of Material Science and Chemical Engineering, Tianjin University of Science and Technology, TEDA, Tianjin 300457, People's Republic of China
Correspondence to: T. Wan (E-mail: wantong@tust.edu.cn)

ABSTRACT: Poly (butylene succinate-*co*-cyclohexanedimethylene succinate) (PBCSs), which are composed of various amounts of cyclohexanedimethylene succinate (CS) with butylene succinate (BS) were synthesized via polycondensation. The composition of PBCSs was analyzed by a ^{1}H-nuclear magnetic resonance (^{1}H-NMR). Crystallization, morphology, and rheological properties of PBCSs were investigated by a polarized optical microscopy (POM), a differential scanning calorimetry (DSC), a X-ray diffraction (XRD), and a parallel-plate rheometer (PPR). The studies revealed that the composition of PBCSs played an important role in controlling their properties. Only one T_g can be seen for PBCSs by DSC, which demonstrate they are miscible copolymers. PBCSs exhibited lower crystallization capacity than its homopolyesters either Poly (butylene succinate) (PBS) or poly (cyclohexanedimethylene succinate) (PCS). It also proved that the cyclohexyl group of CHDM not only affected the crystalline formation, but also changed spherulitic morphology during crystallization. The spherulitic size gradually decreased with an increase of CS content. When CS content approached 50 wt %, the crystallization ability reached minimum. By comparing the effect of temperature with shear rate, it concluded that the viscosities of PBCSs were more sensitive to temperature rather than shear rate, and flow activation energies of PBCSs linearly increased with an increase of CS content. © 2013 Wiley Periodicals, Inc. J. Appl. Polym. Sci. **2014**, *131*, 40103.

KEYWORDS: polyesters; morphology; crystallization; rheology

Received 1 June 2013; accepted 22 October 2013
DOI: 10.1002/app.40103

INTRODUCTION

Biodegradable polyesters have attracted considerable interests in environmental, biomedical, and agricultural applications in recent years.[1–4] They can be biodegraded to natural substances such as CO_2, H_2O, or CH_4 eventually by a wide variety of microorganisms and enzymes without adverse effects on the environment.[5,6] Appropriate design in molecular structure for biodegradable polyesters is still a challenge to meet the requirements of various commercial applications.[7–9] Copolymerization has been recognized as an effective method for enhancing and altering the comprehensive properties. PBS as one of biodegradable polyesters is easily polymerized via esterification and polycondensation of butylene diols with succinic acids (SAs). Its physical properties such as crystalline structure, morphology, crystallization behavior, mechanical property, and rheology can be altered by incorporation of different molecular structures in the repeating units from various diols $HO-R_1-OH$ to various dicarboxylic acids $HOOC-R_2-COOH$.[10–14]

Biodegradable copolyesters can be classified into three categories: aliphatic-*co*-aliphatic, aliphatic-*co*-aromatic, and aliphatic-*co*-alicyclic copolyesters. Aliphatic-*co*-aliphatic copolyesters are developed by copolymerization of various aliphatic diols and aliphatic acids such as poly(butylene succinate-*co*-butylene adipate) PBSA.[15–18] Most of them are full biodegradable, but some disadvantages especially low physical properties and limited processing conditions restrict them to practical applications. The mechanical properties of aliphatic-*co*-aromatic copolyesters are improved by adding aromatic groups to aliphatic backbones such as poly(butylene succinate-*co*-butylene terephthalate) PBST and poly (ethylene succinate-*co*-ethylene terephthalate) PEST, but their biodegradability is deteriorated.[19–22]

The physical properties of PBSA and PBST are compared in detail, because only difference in molecular structure between PBSA and PBST lie on adipate group in PBSA and terephthalate group in PBST. PBSA exhibits a lower crystallization capacity and a lower melting point compared with its homopolyesters either PBS or poly (butylene adipate) (PBA) due to the reduction on the regularity of chain structure. The crystallinity of PBSA reaches minimum value when the content of butylene adipate (BA) unit approaches 50 mol %. Glass transition temperature (T_g) of PBSA shifts to a lower temperature as BA

content increases.[10,23,24] On the contrary, T_g of PBST increases with an increase of butylene terephthalate (BT) content. Their melting point (T_m) and melting enthalpy (ΔH_m) decrease initially by incorporation of a small amount of BT, and then increase when BT content exceeds a critical value at 27.5 mol% of BT content, at which the main crystalline structure of copolyesters changes from PBS to PBT domain.[25] The results conclude that these physical properties of copolyesters can be altered via adjusting the composition of repeating units.

Unlike biodegradable aliphatic-*co*-aliphatic and aliphatic-*co*-aromatic polyesters, which have been extensively investigated, few studies have investigated alicyclic/aliphatic polyesters.[11,12] 1,4-cyclohexanedimethanol (CHDM) containing an alicyclic unit has been widely used for controlling the crystallization and mechanical properties of polyethylene terephthalate (PET). Poly(butylene succinate-*co*-cyclohexanedimethanol succinate) (PBCS), as a typical aliphatic-*co*-alicyclic copolyester, has been synthesized by copolymerization of SA, 1,4-butane diol (BD), and CHDM.[26–29] The biodegradability of this copolyester has been evaluated by enzymatic hydrolysis. Experimental results show that PBCSs are eroded from surface with a random endo-type scission, in which surface hydrophilicity was the predominant effect on enzymatic hydrolysis. Incorporation of a small amount of CS unit into PBS backbone can reduce the regularity of the molecular chains of PBCSs and hence decrease their melting point and crystallinity, while increase the tensile elongation. Thus, considering the film-forming applications, the copolyesters by incorporation of alicyclic units such as CS into PBS backbone turn out to be very interesting. However, their physical properties based on process-ability have not been systematically investigated, especially with various amounts of CS content in an entire composition range. Few work studies the influence of temperature and shear rate on the rheology, so the crucial processing parameters such as viscosities and flow activation energies of PBCSs are analyzed in the present article. The relationships between the composition and the processing properties such as temperature effect on the crystallization and morphology are of interest. We expect that the studies gain herewith could give more knowledge in understanding their physical and processing properties.

EXPERIMENTAL

Materials

SA (98 %) and BD (99 %) were supplied by Shanghai Kefeng chemical reagent. CHDM (98.5%) containing the mixture of *cis*-/*trans*-configuration in the ratio of 1/3, anhydrous Tin (II) chloride (97.5 %), and *p*-toluenesulfonic acid (99 %) were supplied by J&K chemical reagent. All materials were dried at 70°C under vacuum before polymerization.

Synthesis of Poly(butylene succinate-co-cyclohexanedimethylene succinate) (PBCSs)

PBCSs were synthesized using a two-stage polymerization. SA with excess BD in 1/1.2 mole ratio was esterificated at 150°C under a nitrogen gas in the presence of 0.1 wt % catalysts, which is composed of anhydrous Tin (II) chloride anhydrous and *p*-toluenesulfonic acid in 3/2 weight ratio, and then was polycondensed at 220°C under a reduced pressure to 50 mmHg for 2 hours to create butylene succinate (BS). Cyclohexanedimethylene succinate (CS) was created using 1/1.2 mole ratio of SA/CHDM via the same polymerization process as mentioned above. Polycondensation of BS with CS was conducted at 220°C under a vacuum below 5 mmHg for 3–5 hours until the molten copolymers rose up toward the stirring shaft, which is referred to as the weissenberg effect happened at the end. PBCSs with various weight percent of CS (Φ_{CS}) were denoted as PBCS-Φ_{CS}, where Φ_{CS} is 10, 20, 30, 50, 70, 80, 90. Virgin PBS synthesized from BS and virgin poly (cyclohexanedimethylene succinate) (PCS) synthesized from CS using the same polycondensation process were created as references.

Characterization

^{1}H-nuclear Magnetic Resonance. The ^{1}H-nuclear magnetic resonance (^{1}H-NMR) spectra for synthesized PBCSs were recorded by a Bruker Avance 300 MHz spectrometer. All spectra were obtained at 25°C with $CDCl_3$ as a solvent, and tetramethylsilane (TMS) was used as the internal reference.

Gel Permeation Chromatography. The molecular weight (M_n) and polydispersity index (M_w/M_n) of PBSCs were analyzed by a gel permeation chromatography, PL-GPC220 using a refractive index (RI) detector. Chloroform was used as the eluent at a flowing rate of 1.0 mL/min at 40°C, and the concentrations of PBCSs were about 2 mg/mL. Polystyrene standards with low polydispersity were used to make a calibration curve.

Intrinsic Viscosity. The intrinsic viscosity of PBCSs was measured using an Ubbelohde viscometer at 25°C. Each solution was prepared by dissolving 0.04 g PBCSs in 25 mL chloroform.

X-ray Diffraction. X-ray diffraction (XRD) was used to measure the crystalline structure of PBCSs with various CS content at room temperature. XRD patterns were taken on a Philips X′pert Pro (PW3040160) X-ray diffracttometer, using flat plate geometry with Cu Kα radiation (40 kV, 30 mA). The sample films were prepared by a compression molding machine, and were cut to fit the plate aperture. Since their melting point (T_m) various with Φ_{CS}, the sample films were annealed at the temperature, which was lower than their T_m. For PBCS-30, PBCS-50, PBCS-70 which do not present T_c due to slow crystallization rate, they are placed at 30°C for 4 hours in a vacuum oven in order to obtain their crystalline structure. All films were placed into the plate aperture before performing the XRD experiments. Data were collected as step scans from $5^\circ \leq 2\theta \leq 60^\circ$, with a step of 0.02° and a time/step of 1.25 s.

Polarizing Optical Microscope. A Nikon polarizing optical microscope (POM) equipped with a hot stage was used to observe crystalline morphology of PBCSs under the isothermal crystallization process. A small sample weighing about 5 mg was sandwiched between two glass cover slips and placed on a digital hotplate. The hotplate was rapidly heated above T_m of the sample and kept for 3 min. The molten sample was gently pressed between glass cover slips, and then was rapidly cooled to an isothermal crystallization temperature. All samples were isothermally annealed at the temperature, which was 30°C lower than their T_m. For PBCS-30, PBCS-50, PBCS-70, which did not present T_c due to slow crystallization rate, they were annealed at

Table I. Characteristic ^{1}H-NMR Shifts of PBCSs

Type of proton	*position	chemical shift signals (δ), ppm
—O—CH_2*CH_2*CH_2—O—	1	1.71
—C(=O)—CH_2*—CH_2*—C(=O)—	2	2.63
—O—CH_2*CH_2CH_2*CH_2—O—	3	4.12
—C$_6$H$_4$*—	4_{trans}, 4_{cis}	1.00, 1.79
—O—CH_2*—C$_6$H$_4$—CH_2*—O—	5_{trans}, 5_{cis}	4.12, 3.81

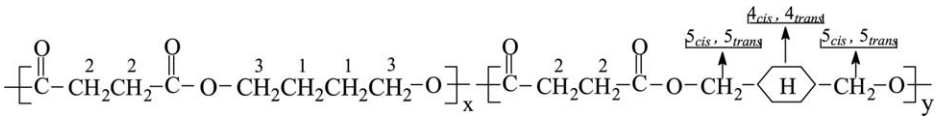

30°C and kept at this temperature for observing the crystalline morphology under crossed polarizer. A CCD camera was used to snap the optical texture images.

Differential Scanning Calorimetry. Thermal properties of PBCSs were studied using differential scanning calorimetry (DSC), DSC 204 F1, NETZSCH. All samples were weighed between 5 and 10 mg accurate to 0.1 mg. The first heating process was performed from −50 to 140°C with 5°C/min of heating rate, and then annealed for 3 min to eliminate the thermal history. The cooling process was performed from 140 to −50°C with 5°C/min of cooling rate, and then a second heating process was performed from −50 or −70 to 140°C with 5°C/min of heating rate again. All data were analyzed by TA Universal Analysis 2000.

Parallel-Plate Rheology. Rheology measurements were conducted on a HAKKE MARS III Rheometer. All tests were performed at 130°C and loaded into a pair of parallel plates with 25 mm in diameter and 1-mm gap size. For oscillatory shear studies, a sinusoidal strain in the form of $\gamma(t) = \gamma_0 \sin(\omega t)$ was applied, and the torque force was recorded by a sensor and converted to the elastic modulus G' in phase and the viscous modulus G'' out of phase. The angular frequency sweep ranged from 0.5 to 100 rad/s at low strain amplitude to ensure that the measurements were taken well within the linear viscoelastic range. For steady viscosity measurement, the applied shear rate ranges from 0.5 to 100 rad/s. Sample disks with 25 mm in diameter and 1 mm in thickness were prepared by a compression molding machine.

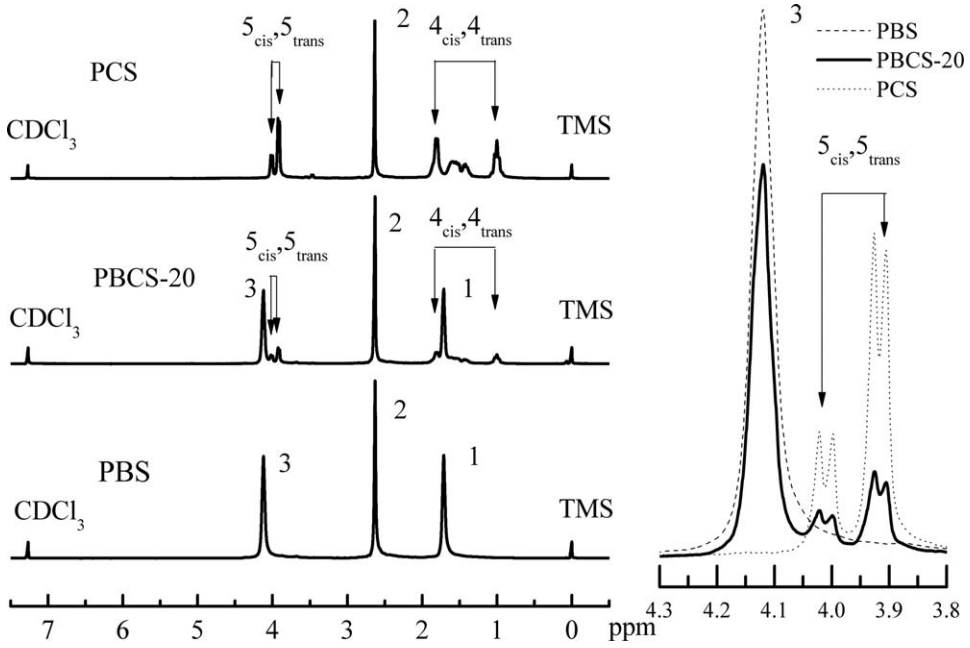

Figure 1. The ^{1}H-NMR spectra of PBCS-20, PCS, and PBS.

Table II. Composition and Molecular Weight and Polydispersity Index and Intrinsic Viscosities of PBCSs

Sample name	Φ_{CS}[a]	W_{CS}[b]	$M_{BS/CS}$[c]	$M_n \times 10^{-4}$ (g/mol)	Mw/Mn	$[\eta]$[d] (dL/g)
PBS	0	0	-	4.1	2.17	1.09
PBCS-10	10	0.18	5.98	3.8	2.23	0.99
PBCS-20	20	0.31	2.92	4.2	2.22	1.13
PBCS-30	30	0.40	1.97	4.9	2.41	1.01
PBCS-50	50	0.55	1.08	5.8	2.61	1.18
PBCS-70	70	0.75	0.44	4.2	2.39	1.08
PBCS-80	80	0.87	0.31	3.5	2.31	1.02
PCS	100	1	-	2.8	2.08	1.13

[a] Φ_{CS} represents feeding amount of CS in the weight percent.
[b] W_{CS} represents the weight percent of CS in the copolymers calculated from ^{1}H-NMR spectra.
[c] $M_{BS/CS}$ represents mole ratio of BS unit to CS unit calculated from ^{1}H-NMR spectra.

RESULTS AND DISCUSSION

The Composition of PBCSs

The ^{1}H-NMR spectra of PBCSs with various Φ_{CS} are analyzed and the chemical shift signals of the protons are shown in Figure 1 and Table I. Figure 1 shows the ^{1}H-NMR spectrum of PBS exhibits three main characteristic peaks located at 1.71 ppm, 2.63 ppm, and 4.12 ppm.[30] The chemical shift signals of the protons in methylene groups of $-O-\overset{3}{C}H_2\overset{1}{C}H_2\overset{1}{C}H_2\overset{3}{C}H_2-O-$ correspond to $\delta = 1.71$ ppm (d, H^1) and $\delta = 4.12$ ppm (d, H^3). The peak at $\delta = 2.63$ ppm (d, H^2) is assigned to the protons in methylene groups of $-\overset{O}{\overset{\|}{C}}-\overset{2}{C}H_2\overset{2}{C}H_2-\overset{O}{\overset{\|}{C}}-$. The assignments of *cis*- and *trans*−1,4-cyclohexanedimethylene groups in $CDCl_3$ are obtained from the ^{1}H-NMR spectrum of PCS. Signals corresponding to the chemical shift of the protons in $-\langle\overset{4_{cis},\,4_{trans}}{H}\rangle-$ containing *cis*- and *trans*-conformation are observed at $\delta = 1.00$ ppm (d, $H^{4_{trans}}$) and $\delta = 1.79$ ppm (d, $H^{4_{cis}}$). The signals at $\delta = 3.81$ ppm (d, $H^{5_{trans}}$) and $\delta = 4.12$ ppm (d, $H^{5_{cis}}$) represent the protons in methylene groups of $-O-\overset{5_{cis},\,5_{trans}}{CH_2}-\langle H\rangle-\overset{5_{cis},\,5_{trans}}{CH_2}-O$, which are attached to the ester groups. The composition of PBCSs can be calculated from their peak area (I_H) of the protons. The peak area ratio ($I_H^{5_{cis}}/I_H^{5_{trans}}$) is 1/3 in all compositions of PBCSs, since CHDM is a mixture composed of *cis*- and *trans*-configuration. The peak area ratio (I_H^3/I_H^5) increases with an increase of Φ_{CS}. The real weight percent of CS in PBCSs (W_{CS}) can be calculated according to eq. (1).

$$W_{CS} = \frac{(I_H^{5_{trans}}/4 + I_H^{5_{cis}}/4)\times 226}{(I_H^3/4)\times 172 + (I_H^{5_{trans}}/4 + I_H^{5_{cis}}/4)\times 226} \quad (1)$$

The relative mole ratio of BS to CS unit ($M_{BS/CS}$) can be determined according to eq. (2).

$$M_{BS/CS} = \frac{226\times(1-W_{CS})}{172\times W_{CS}} \quad (2)$$

where $I_H^{5_{trans}}/I_H^{5_{cis}}$ and designate the peak areas of the methylene protons in *cis*- and *trans*-configuration of CHDM respectively. I_H^3 designates the peak area of the methylene protons of BD. W_{CS} is the real weight percent of CS in PBCSs. The molecular weight of a CS unit and a BS unit are 226 and 172, respectively.

The composition of PBCSs with various amounts of Φ_{CS} is summarized in Table II. Compared with the feeding amount of CS, its real weight percent in the copolymer always presents a higher value. During the polycondensation process, the boiling point of BD (228°C, 760 mmHg) is lower than that of CHDM (283°C, 760 mmHg), so BD is easier to be extracted than CHDM, which results in Φ_{CS} values are slightly lower than that of W_{CS}. To simplify this analysis, this article adopts Φ_{CS} values as the change of CS content to characterize the performance of PBCSs.

Table II shows the effect of different CS content on the number-average molecular weight (M_n) and polydispersity index (M_w/M_n) of the copolymers. The number-average molecular weight obtained from GPC is various from 2.8×10^4 to 5.8×10^4 g/mol by the introduction of CS and polydispersity indexes of PBCSs copolymer are in the range of 2.17–2.61. When the feeding weight percent of CS is lower than 50%, the molecular weight of PBCSs first slightly increases with an increase of CS content. PBCS-50 has a maximum molecular weight ($M_n = 5.8 \times 10^4$ g/mol) among the all samples. The achieved high molecular weight values could probably be attributed to the high vacuum applied during the polycondensation step. However, when CHDM feeding amount is higher than 70%, the molecular weight obviously decreases. In particular, PCS exhibits a lowest number-average molecular weight (M_n) among all samples. Due to a higher boiling temperature, CHDM is more difficult to be extracted than BD during the vacuum pumping process resulting in the change of molecular weight of PBCSs, showing a clear downward trend.

XRD Analysis

To investigate the effect of Φ_{CS} on the crystalline structure of PBCSs, XRD measurements were conducted in the range of 5–60°. Figure 2 shows the crystalline patterns of PBS, PBCSs, and PCS for comparison. PBS exhibits three main characteristic diffraction peaks located at 19.8°, 22.2°, and 22.8°, which are attributed to (020), (021), and (110) planes of the crystallites.[31]

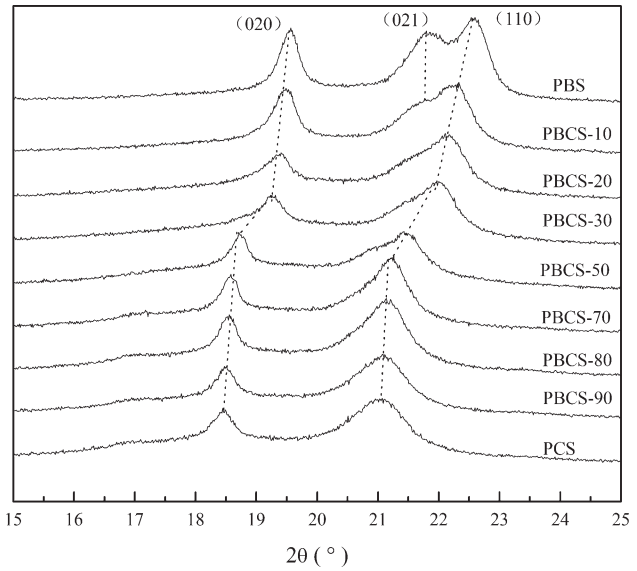

Figure 2. XRD patterns of PBCSs with various Φ_{CS}.

As shown in Figure 2, neat PCS presents two strong characteristic diffraction peaks at 18.4° and 21.1°. With the increase of CS content, the main characteristic diffraction peaks of PBCSs are shifted toward low angle, indicating the reduction of crystalline size of the copolymer by the incorporation of CS. According to their peak position, the crystalline structures can be divided into PBS crystalline domain and PCS crystalline domain. PBS crystalline lattice predominates for PBS, PBCS-10, PBCS-20, and PBCS-30. On the contrary, at the high CS content, PBCS-70, PBCS-80, and PBCS-90 presenting slightly peak shifts indicate PCS crystalline domain regardless of the composition variation. PBCS-50 exhibits intermediate crystalline structure between both of two crystalline domains.

Crystalline Morphology of PBCSs

The crystallization behavior and crystalline morphology are also related to their compositions. Figure 3 shows these PBCSs exhibit two typical crystalline morphologies. PBS, PBCS-10, and PBCS-20 present the ring-banded spherulites with Maltese cross. The ring-banded texture is a typical feature in some major biopolyesters such as PBS, polycaprolactone (PCL), and polyhydroxybutyrate (PHB) and their copolymers due to periodically rotation of the chain axis around a radial direction.[32–34] However, the perfection of ring-banded spherulites is undermined and the regular concentric arrangement disappears with a further increase of Φ_{CS} such as PBSC-30. PBCS-50 contains very rare crystalline textures due to its low crystallization capacity during an observation period. It should be noted that, although PBCS-50 does not display the crystalline texture due to a very low crystallization rate, it is nevertheless still a semicrystalline polyester. At the high CS content, PBCS-70, PBCS-80, PBCS-90, and PCS present very small similar sized spherulites without

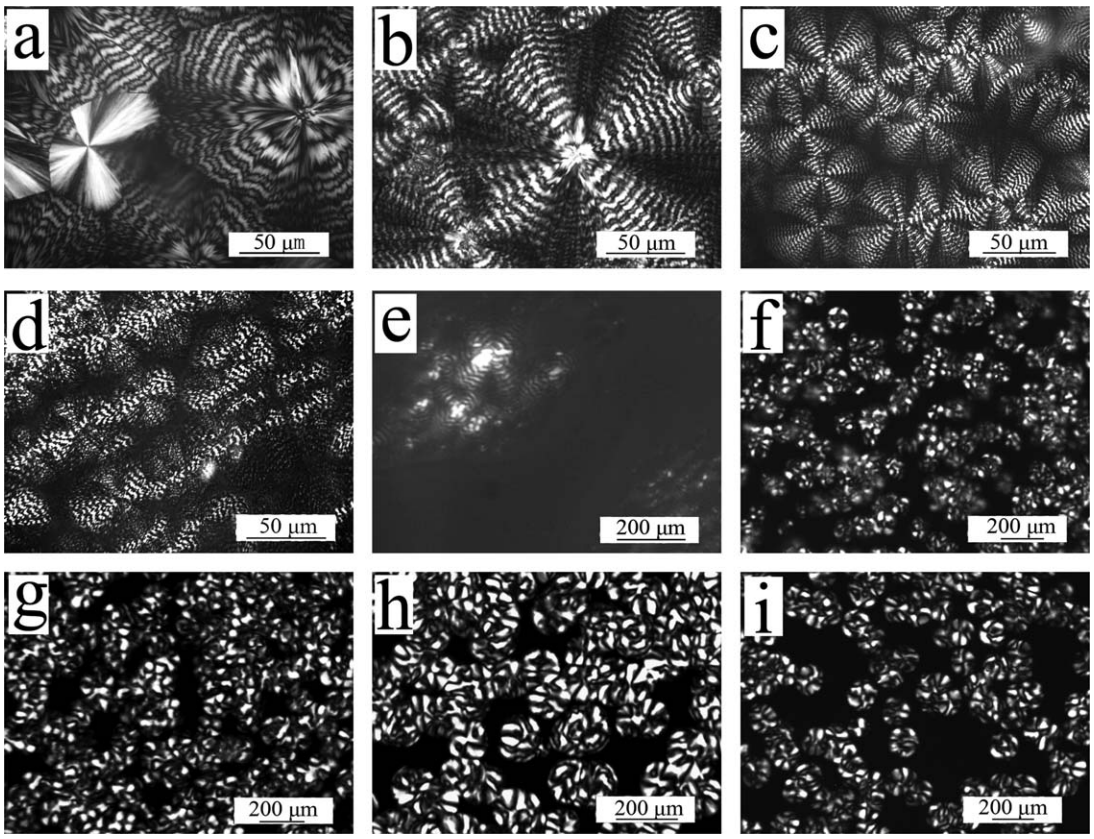

Figure 3. Polarized optical micrographs of crystallized PBCSs. (a) PBS; (b) PBSC-10; (c) PBSC-20; (d) PBSC-30; (e) PBSC-50; (f) PBSC-70; (g) PBSC-80; (h) PBSC-90; and (i) PCS.

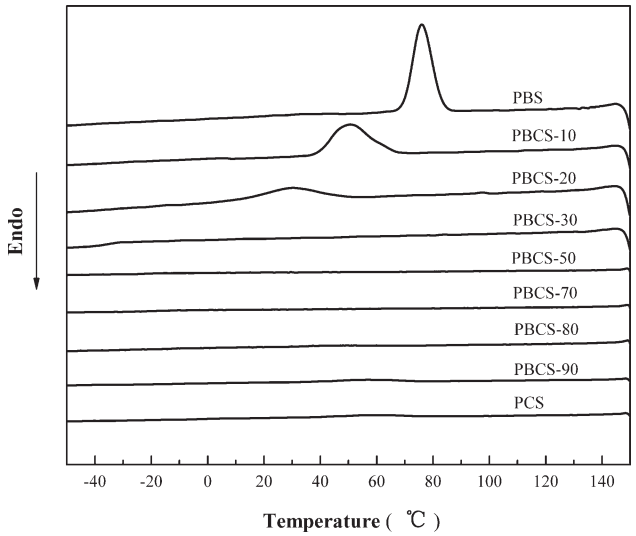

Figure 4. DSC thermograms of PBCSs under the cooling scan.

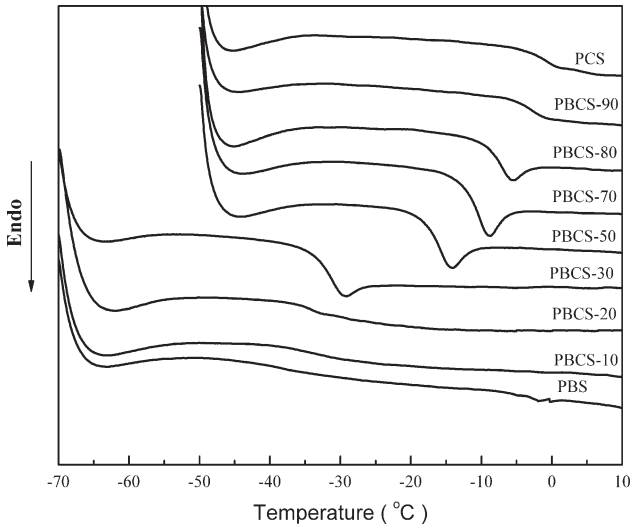

Figure 6. Glass transition temperature (T_g) of PBCSs

ring-banded feature. According to crystalline structure and morphology analysis, it indicates that ring-banded spherulites of PBCSs at low Φ_{CS} presenting PBS crystalline domain, while regular spherulites of PBCSs at high Φ_{CS} present PCS crystalline domain. It also proves that the cyclohexyl group of CHDM not only affects the crystalline formation, but also changes of spherulite morphology during crystallization.

Thermal Properties

The composition variation of PBCSs alters their thermal properties; furthermore, it influences their processibility. Figure 4 presents the cooling thermograms of PBS, PBCSs, and PCS from 140 to −50°C. The hot crystallization temperature (T_c) of PBCSs decreases with an increase of Φ_{CS} for PBCS-10, PBCS-20, and PBCS-30. No significant exothermic peak can be found with a further increase of Φ_{CS} for PBCS-50 and PBCS-70, PBCS-80, and PBCS-90 due to a very low crystallization rate.

Figure 5 shows the melting behaviors of PBS, PBCSs, and PCS from −50 to 140°C in the heating thermograms. PBS exhibits a

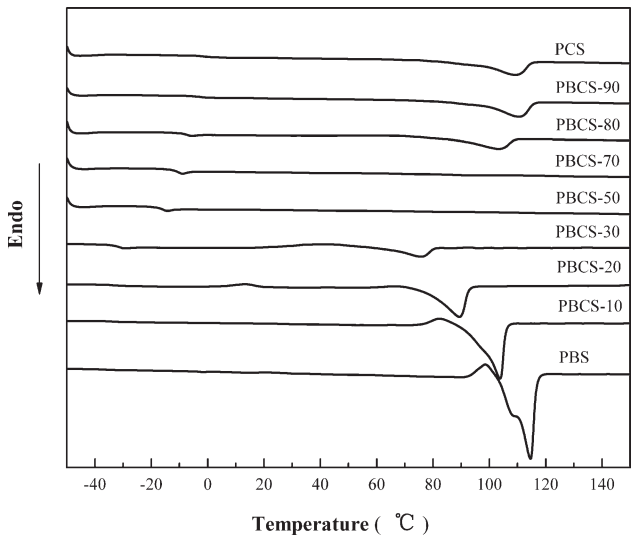

Figure 5. DSC thermograms of PBCSs under the heating scan.

melting point (T_m) at 115°C, which is in agreement with previous studies.[35] PCS exhibits a lower T_m at 110°C, and a smaller endothermic peak compared with PBS. With an increase of Φ_{CS} for PBCS-10, PBCS-20, and PBCS-30, the melting point (T_m) decreases, but for PBCS-80 and PBCS-90 only small endothermic peak which is similar to that of PCS can be observed. The Figure 6 enlarges the lower temperature region from −70 to 10°C to clearly observe their glass transition temperature (T_g). The variation in T_g and thermal properties of PBCSs is summarized in Table III. T_g of PBS is −35°C, which is similar with Tsai's report.[26] PCS has a highest T_g at −1°C among all samples. PBCSs exhibit an intermediate behavior depending on their composition. As seen from Table III, T_g increases from −35 to −1°C with an increase of CS content. Only one T_g can be observed for PBCSs by DSC, so they are miscible copolymers. The increment trend also complies with Flory-Fox theory about T_g approximation. It can be attributed to the presence of cyclohexyl group in CS unit, which decreases their T_g.

PBS exhibits a large melting enthalpy at 115°C and a higher degree of crystallinity, while neat PCS presents a small melting enthalpy at 105°C indicating a rather low cold crystallization capacity. By comparison of neat PBS and PCS, the T_c and the crystallization enthalpy (ΔH_c) of PBCSs shift toward lower value. The melting point (T_m) and melting enthalpy (ΔH_{m1} or ΔH_{m2}) first decrease gradually with an increase of Φ_{CS}, but then both of them increase again. In the case of PBCS-50, it is hardly to observe its melting point (T_m) and melting enthalpy (ΔH_{m1} or ΔH_{m2}), indicating the introduction of a cyclohexyl group greatly reduces the crystallization rate. PBCSs with over 70 wt % of Φ_{CS} still show relative high melting point and small crystallization enthalpy. The regularity of main chain is an important parameter for the polymer's capacity to crystallize. A small addition of CHDM undermines the crystallization integrity of PBS, so the crystallinity and crystallization rate of PBCSs are reduced. When the CS content close to 50 wt %, crystallization rate becomes very slowly, in other word, no crystallization peak for PBCS-50 and PBCS-70 can be observed in DSC

Table III. Thermal Properties of PBCSs

	T_g (°C)	ΔH_c[a] (J/g)	T_c[b] (°C)	ΔH_{m1}[c] (J/g)	T_{m1}[d] (°C)	ΔH_{m2}[e] (J/g)	T_{m2}[f] (°C)
PBS	−35	−70.6	76.1	74.2	114.6	74.2	114.1
PBCS-10	−34	−47.2	50.6	55.0	103.8	53.0	103.5
PBCS-20	−33.5	−29.6	29.5	39.3	89.4	46.3	89
PBCS-30	−31.8	-	-	6.92	75.8	14.9	75.4
PBCS-50	−16.5	-	-	-			-
PBCS-70	−10.3	-	-	0.8	94.9		
PBCS-80	−7.7	-	35	20.6	103.3	28.7	104.9
PBCS-90	−3.5	−23.7	56.9	29.3	109.5	30.4	110.3
PCS	−1.1	−24.2	58.8	111.1	111.1	31.2	111.9

[a] ΔH_c represents crystallization enthalpy.
[b] T_c represents crystallization temperature in cooling scan.
[c] ΔH_{m1} represents melting enthalpy in the first heating scan.
[d] T_{m1} represents melting point in the first heating scan.
[e] ΔH_{m2} represents melting enthalpy in the second heating scan.
[f] T_{m2} represents melting point in the second heating scan.

thermograms with 5°C/min cooling scan. However, their crystallization ability increases with a further increase of CS up to the major part, due to PCS structure are also crystallizable for PBCS-80, PBCS-90 and PCS. The glass transition temperatures (T_g) of all samples are lower than the room temperature, so these samples can crystallize at the room temperature over a period of time. It is not a contradiction with the observation from Figure 2. Even though the crystallization and melting behaviors can not be observed for PBCS-30, PBCS-50, and PBCS-70 during cooling process due to the limitation of ramping time in DSC, XRD patterns and crystalline morphologies measured from XRD and polarized optical microscopy (POM) demonstrate they are still crystallizable, but a relative longer annealing time is needed to form crystallites.

Due to a long time annealing, the samples for XRD measurement undergo the slow crystallization. The XRD results from Figure 2 can well explain the difference in the crystalline structures, while Figure 5 demonstrates the variation of crystallization ability of various PBCSs. It proves that the cyclohexyl group of CHDM not only affects spherulite morphology and crystallinity of copolymers but also alters crystallization and melting behaviors.

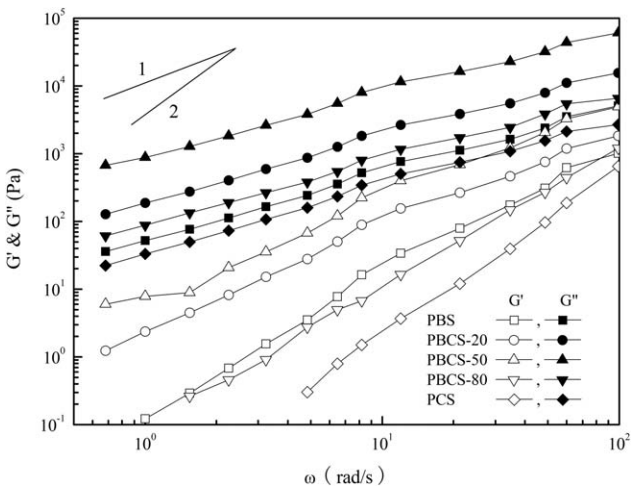

Figure 7. Elastic modulus (G') and viscous modulus (G'') of PBCSs with various Φ_{CSO} as a function of angular frequency (ω) at 130°C.

Rheology of PBCSs

Elastic modulus (G') and viscous modulus (G'') of PBCSs with various Φ_{CS} as a function of angular frequency (ω) at 130°C are plotted in Figure 7. The opened symbols represent G' and closed symbols represent G'' respectively. The curve slope reflects flow behaviors. The values of G' are orders of magnitude lower than the corresponding G'' over the applied frequencies for all samples, implying that the melts exhibit good flowabilities. PBCSs exhibit a liquid-like flow behavior, because G' is nearly proportional to ω^2 and G'' is proportional to ω. G' and G'' increase with the incorporation of CS unit into PBS backbone until Φ_{CS} approaches 50 wt %. However, the further addition of CS (>50 wt %) in PBCSs results in a decrease of both G' and G'', but slightly alters the curve slope. The curve slopes of G'' for all PBCSs versus ω are nearly unity in the measured range, indicting their complex viscosities are independent of angular frequency, and further implying the viscosities of all PBCSs are not sensitive to shear rate. On the other hand, the slopes of G' are considerably lower for all PBCSs compared with those of neat PBS and PCS, while the slopes of G'' are invariable regardless of the composition variation.

To understand the steady shear rheological behavior of PBS, PCS, and a series of PBCSs the viscosities versus shear rate are shown in Figure 8. The viscosities of all PBCSs, including PBS, and PCS exhibit nearly Newtonian plateau in a broaden shear region from 0.01 to 10 s^{-1} and only slightly decrease at higher shear rates, so their viscosities are not sensitive to the shear rate regardless of the composition variation. The similar behavior is observed for biodegradable polymers like PCL and aliphatic polyester (BAP).[36,37] The curves for all PBCSs have almost identical shape to that obtained for neat PBS or PCS, with the exception of viscosity variation. When shear rate increases beyond 10 s^{-1}, PBCSs exhibit slightly pseudoplastic behavior,

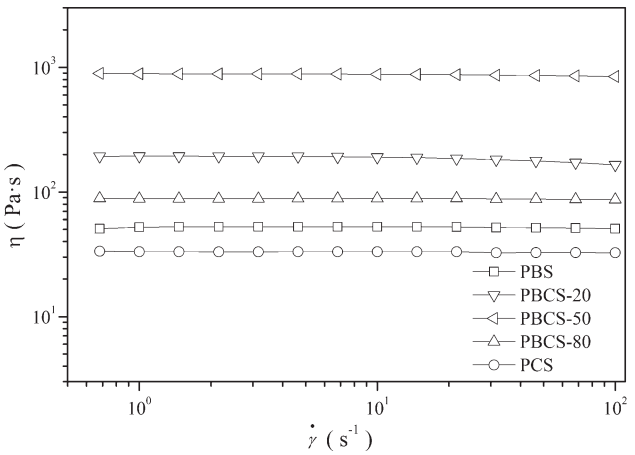

Figure 8. Viscosities (η) of PBCSs with various Φ_{CS} as a function of shear rate at 130°C.

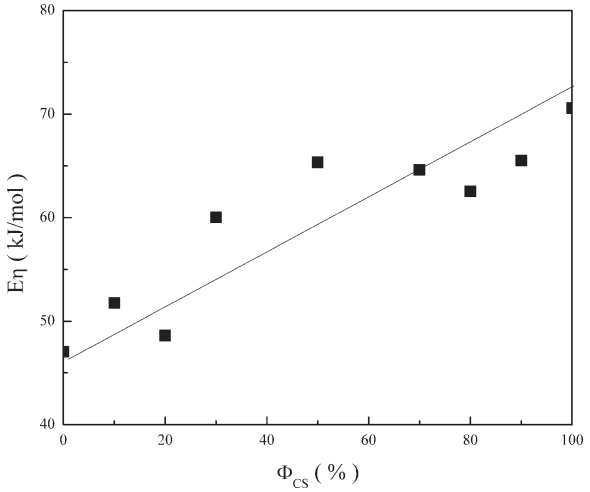

Figure 9. Flow activation energy of PBCSs (E_η^{PBCS}) with various Φ_{CS}.

but PBS still exhibits Newtonian behavior. All PBCSs show a very strong Newtonian plateau behavior below 10 s^{-1} and this behavior is analogous to the results obtained in the case of oscillatory shear measurements.

Zero viscosity (η_0) of PBCSs exhibit a fluctuation with Φ_{CS}. With an increase of Φ_{CS}, the viscosities first increase significantly, but then decrease again above a critical value at 50 wt % of Φ_{CS}. However, PBCSs are copolyesters which show miscibility in molecular level. The change of viscosity strongly depends on the variation of molecular weight and polydispersity. GPC analysis gives a clear trend to prove the variation of viscosity for PBCSs. When CS content is lower than 50%, the molecular weight of polyester slightly increased with the increasing of CS content. The achieved high molecular weight values could probably be attributed to the high vacuum applied during the polycondensation step. PBCS-50 has a maximum molecular weight among all samples. However, when CS feeding amount is higher than 70%, the molecular weight obviously decreased, because CHDM is more difficult to be extracted than BD during the vacuum pumping process resulting in a clear downward trend of molecular weight. Thus, η_0 strongly depends on the various compositions of PBCSs and vacuum applied.

Flow activation energy for flow (E_η) of PBCSs has been studied to evaluate their temperature susceptibility. Zero viscosities of PBCSs at various temperatures are selected from Newtonian plateau. The flow activation energy of PBS (E_η^{PBS}) is around 46 kJ/mol, which is in agreement of previous results,[38] while PCS shows a higher flow activation energy (E_η^{PCS}) at 70 kJ/mol. The flow activation energy of PBCSs (E_η^{PBCS}) increases with Φ_{CS} and exhibits an intermediate value between 46 and 70 kJ/mol. An empirical mixture rule can be applied to describe E_η^{PBCS} of PBCSs according to eq. (3).

$$E_\eta^{PBCS} = E_\eta^{PBS} + E_\eta^{PCS}\Phi_{CS} \quad (3)$$

where Φ_{CS} is the weight percent of CS. E_η^{PBCS}, E_η^{PBS}, and E_η^{PCS} represent the flow activation energy of PBCSs, PBS, and PCS flows. Figure 9 shows that E_η^{PBCS} is predicted by plotting a straight line according to eq. (3). The predicted E_η^{PBS} and E_η^{PCS} are 44.5 and 71.9 kJ/mol respectively, which is comparable with the experimental data. The mixture rule qualitatively represents the linearly dependent of Φ_{CS}. By comparing Figures 8 and 9, the viscosities of PBCSs are more sensitive to temperature rather than shear rate.

CONCLUSIONS

PBCSs with various Φ_{CS} were synthesized via a two-stage polymerization: esterification and polycondensation. The chemical composition of PBCS played an important role in controlling their physical properties. All PBCSs were miscible copolymers, because they exhibited only one T_g, which was increased with CS content. Both PBS and PCS had their own crystalline structure, while the main crystalline structure of PBCSs changed from PBS crystalline domain to PCS crystalline domain as the CS content increased. The crystallinity decreased and then increased with incorporation of CS and approached minimum at 50 wt % of Φ_{CS}. PBS exhibited ring-banded spherulites, but PCS had small regular spherulites. The melting point, the melting enthalpy, the spherulitic size of PBCSs decreased gradually with an increase of CS content up to 50 wt %. When CS content further increased above this value, these corresponding properties showed an opposite trend. E_η^{PBCS} linearly increased with an increase of Φ_{CS}. By comparing the effect of temperature and shear rate on their viscosities, it concluded that molten PBCSs were more sensitive to temperatures rather than shear rate.

ACKNOWLEDGMENTS

The authors gratefully acknowledge support from the Scientific Research Foundation for the Returned Overseas Chinese Scholars, (SRF for ROCS) and the Scientific Research Foundation of Tianjin University of Science & Technology (Grant Number: 20080421).

REFERENCES

1. Ikada, Y.; Tsuji, H. *Macromol. Rapid. Commun.* **2000**, *21*, 117.
2. Webb, A. R.; Yang, J.; Ameer, G. A. *Exp. Opin. Biol. Ther.* **2004**, *4*, 801.

3. Mohamed, F.; van der Walle, C. F. *J. Pharm. Sci.* **2008**, *97*, 71.
4. Breitenbach, A.; Li, Y. X.; Kissel, T. *J. Control. Release* **2000**, *64*, 167.
5. Kaith, B.; Kaur, I. Cellulose Fibers: Bio-and Bano-Polymer Composites: Green Chemistry and Technology; Springer: New York, **2011**.
6. Chiellini, E.; Gil, H.; Braunegg, G.; Buchert, J.; Gatenholm, P.; van der Zee, M. Biorelated Polymers: Sustainable Polymer Science and Technology; Kluwer Academic/Plenum Publishers: New York, **2001**.
7. Nayak, P. L. *J. Macromol. Sci. Polym. Rev.* **1999**, *33*, 481.
8. Philip, S.; Keshavarz, T.; Roy, I. *J. Chem. Technol. Biot.* **2007**, *82*, 233.
9. Avella, M.; De Vlieger, J. J.; Errico, M. E.; Fischer, S.; Vacca, P.; Volpe, M. G. *Food. Chem.* **2005**, *93*, 467.
10. Nikolic, M. S.; Djonlagic, J. *Polym. Degrad. Stabil.* **2001**,*74*, 263.
11. Pepic, D.; Zagar, E.; Zigon, M.; Krzan, A.; Kunaver, M.; Djonlagic, J. *Eur. Polym. J.* **2008**, *44*, 904.
12. Ki, H.; Park, O. O. *Polymer* **2001**, *42*, 1849.
13. Tuominen, J.; Seppälä, J. V. *Macromolecules* **2000**, *33*, 3530.
14. Albertsson, A. C.; Varma, I. K. Degradable Aliphatic Polyesters; Springer: New York, **2002**.
15. Shi, F.; Gross, R. A.; Rutherford, D. R. *Macromolecules* **1996**, *29*, 10.
16. Magnusson, H.; Malmström, E.; Hult, A.; Johansson, M. *Polymer* **2002**, *43*, 301.
17. Cao, A.; Okamura, T.; Nakayama, K.; Inoue, Y.; Masuda, T. *Polym. Degrad. Stab.* **2002**, *78*, 107.
18. Ishii, M.; Okazaki, M.; Shibasaki, Y.; Ueda, M.; Teranishi, T. *Biomacromolecules* **2001**, *2*, 1267.
19. Li, F. X.; Xu, X. J.; Hao, Q. H.; Li, Q. B. Yu, J. Y.; Cao, A. *J Polym. Sci. Part B: Polym. Phys.* **2006**, *44*, 1635.
20. Bikiaris, D. N.; Papageorgiou, G. Z.; Achilias, D. S. *Polym. Degrad. Stab.* **2006**, *91*, 31.
21. Chuah, H. H. *Macromolecules* **2001**, *34*, 6985.
22. Deng, L. M.; Wang, Y. Z.; Yang, K. K.; Wang, X. L.; Zhou, Q.; Ding, S. D. *Acta. Mater.* **2004**, *52*, 5871.
23. Montaudo, G.; Rizzarelli, P. *Polym. Degrad. Stab.* **2000**, *70*, 305.
24. Rizzarelli, P.; Puglisi, C.; Montaudo, G. *Polym. Degrad. Stab.* **2004**, *85*, 855.
25. Gan, Z.; Kuwabara, K.; Yamamoto, M.; Abe, H.; Doi, Y. *Polym. Degrad. Stab.* **2004**, *83*, 289.
26. Tsai, Y.; Jheng, L. C.; Hung, C. Y. *Polym. Degrad. Stab.* **2010**, *95*, 72.
27. Jung, I. K.; Lee, K. H.; Chin, I. J.; Yoon, J. S.; Kim, M. N. *J. Appl. Polym. Sci.* **1999**, *72*, 553.
28. Lecomte, H. A.; Liggat, J. J.; Curtis, A. S. *J. Polym. Sci. Part A: Polym. Chem.* **2006**, *44*, 1785.
29. Zhu, C.; Zhang, Z.; Liu, Q.; Wang, Z.; Jin, J. *J. Appl. Polym. Sci.* **2003**, *90*, 982.
30. Huang, C. L.; Jiao, L.; Zhang, J. J.; Zeng, J. B.; Yang, K. K.; Wang, Y. Z. *Polym. Chem.* **2012**, *3*, 800.
31. Tserki, V.; Matzinos, P.; Pavlidou, E.; Vachliotis, D.; Panayiotou, C. *Polym. Degrad. Stab.* **2006**, *91*, 367.
32. Jiang, S.; He, C.; An, L.; Chen, X.; Jiang, B. *Macromol. Chem. Phys.* **2004**, *205*, 2229.
33. Yang, J.; Pan, P.; Hua, L.; Xie, Y.; Dong, T.; Zhu, B.; Inoue, Y.; Feng, X. *Polymer* **2011**, *52*, 3460.
34. Chang, L.; Woo, E. *Polymer* **2011**, *52*, 68.
35. Qiu, Z.; Miao, L.; Yang, W. *J. Polym. Sci. Part B: Polym. Phys.* **2006**, *44*, 1556.
36. Ramkumar, D.; Bhattacharya, M. *Polym. Eng. Sci.* **1998**, *38*, 1426.
37. Shin, T. K.; Kim, J.; Choi, H. J.; Jhon, M. S. *J. Appl. Polym. Sci.* **2000**, *77*, 1348.
38. Sinha Ray, S.; Okamoto, K.; Okamoto, M. *Macromolecules* **2003**, *36*, 2355.